UREA EQUILIBRIUM UNFOLDING OF THE MAJOR CORE PROTEIN OF THE RETROVIRUS FELINE IMMUNODEFICIENCY VIRUS AND ITS TRYPTOPHAN MUTANTS

Running Title: Unfolding of FIV-rp24

Belén Yélamos [a], Elena Núñez [a], Julián Gómez-Gutiérrez [a], Carmen Delgado [a], Beatriz Pacheco [a], Darrell L. Peterson [b] and Francisco Gavilanes [a,*]

[a] Departamento de Bioquímica y Biología Molecular I. Facultad de Ciencias Químicas. Universidad Complutense de Madrid. 28040 Madrid, Spain.

[b] Department of Biochemistry and Molecular Biophysics. Virginia Commonwealth University. Richmond. 23298 Virginia, USA.

*Corresponding author: F. Gavilanes, Departamento de Bioquímica y Biología Molecular I. Facultad de Ciencias Químicas. Universidad Complutense de Madrid. 28040 Madrid, Spain. Fax: + 34 91 394 4159. Tel.: + 34 91 394 4266
e-mail: pacog@bbm1.ucm.es

Keywords: FIV core protein; tryptophan mutants; site-directed mutagenesis; urea denaturation; folding intermediates.

Abbreviations: CD, circular dichroism; EIAV, equine infectious anemia virus; F_{app}, apparent fraction of the unfolded protein; FIV, feline immunodeficiency virus; FIV-rp24, recombinant FIV p24 protein; *I*, intermediate state; *N*, native structure; *U*, unfolded structure; W40F, recombinant p24 protein with Phe at position 40 instead of Trp; W126F, recombinant p24 protein with Phe at position 126 instead of Trp; W40/126F, recombinant p24 protein with Phe at positions 40 and 126 instead of Trp; [Θ], molar ellipticity.

Abstract

Circular dichroism and fluorescence spectroscopy have been employed to study the urea unfolding mechanism of a recombinant form of the major core protein of feline immunodeficiency virus (FIV-rp24) and its native tryptophan mutants. The equilibrium denaturation curves indicate the existence of two transitions. The first unfolding transition most likely reflects the denaturation of the carboxy-terminal region of FIV-rp24. Consequently, the second transition, where the changes in fluorescence are produced, should reflect the denaturation of the amino-terminal region. If the intermediate observed upon urea denaturation is an on-pathway species, the data described herein can reflect the sequential and independent loss of structure of the two domains that this type of proteins possesses.

1. Introduction

Feline immunodeficiency virus (FIV) is a member of the lentivirus group of the family *Retroviridae.* To this family also belong, among others, the equine infectious anemia virus (EIAV), simian immunodeficiency virus and human immunodeficiency virus (HIV). The viral genome of these viruses is located inside a core structure. The lentiviral major core proteins (so-called p24 or p26 depending on the virus) show a great homology among each other [1-4]. This high degree of amino acid similarity, combined with immunological cross-reactivities and conserved function, suggested that the three-dimensional structure of the lentiviral core proteins was likely related. In fact, the core proteins of EIAV and HIV have been shown to possess the same overall three-dimensional structure being organized into two domains linked by a flexible extended peptide [5-9]. The N-terminal domain (residues 1-151) has a compact bullet shape composed of five coiled-coil α-helices, with two additional short α-helices following an extended proline-rich loop [5,6]. The C-terminal domain (residues 152-231) has four bundled α-helices and an extended strand [7]. The EIAV protein crystallizes as dimers with head-to-head interactions [8] while the dimers observed in crystals of HIV capsid protein complexed with a monoclonal antibody Fab have head-to-tail interactions [9]. The two domains are interconnected by an extended peptide forming a flexible linked dumb-bell-shaped molecule [9].

Initially, this protein is synthesized as part of the polyprotein Gag precursor that assembles into immature virions at the cell membrane [4]. After proteolytic cleavage of the precursor molecule, which takes place during or after budding

from the host cell membrane, the core protein self-associates to form the mature capsid that encloses the viral RNA [10]. Numerous studies have revealed the different roles the two domains play in the formation of the core structure. Thus, mutations in the C-terminal domain affect Gag oligomerization and viral assembly [11,12] while mutations and deletions in the N-terminal domain give rise to virions that assemble but are non-infectious [13, 14]. However, little is known about the way the protein reaches its native structure. The folding of p24 may occur in a single step with the two domains folding cooperatively or proceed through one or more intermediates. Since the interactions between the two domains are weak [9], a multiple transition pathway seems more plausible [15]. The presence of an intermediate can be inferred from a HIV-1 p24 conformational stability study since the recombinant protein isolated from inclusion bodies under strong denaturing conditions has the spectral features of a molten globule state at low pH [16]. To shed more light on the folding mechanism of retroviral capsid proteins, a recombinant capsid protein of FIV has been obtained [17]. This protein, which is 223 amino acids long, has two tryptophan residues at positions 40 and 126 that have been replaced by phenylalanine by site directed mutagenesis to obtain two single mutants and a double mutant. Replacement of one or two tryptophan residues in the protein changes neither the secondary structure elements nor the overall three-dimensional structure of p24 [17]. Consequently, these recombinant proteins are suitable candidates for studies of unfolding-refolding in order to understand how p24 reaches its three-dimensional structure. The urea-induced denaturation of the wild-type and tryptophan mutant proteins has been studied by circular dichroism and emission fluorescence, and the denaturation curves

obtained have been analyzed in terms of the denaturant binding model [18].

2. Materials and methods

2.1. Chemicals

Ultrapure urea was obtained from USB. Sepharose CL-6B Ni-nitrilotriacetic acid (NTA) was purchased from Qiagen. Restriction enzymes, polymerases and other molecular biology reagents were obtained from New England Biolabs. All other reagents were from Merck and Sigma.

2.2. Cloning, expression and purification of FIV-rp24 and tryptophan mutants

The cDNA that codes for the major core protein of FIV was cloned as described previously into the expression vector pQE60 (Qiagen) that adds a six histidines sequence at the carboxy-terminal end of the protein [17]. Site-directed mutagenesis was employed to obtain the two single tryptophan mutants, W40F and W126F, and a double mutant, W40/126F [17].

All the recombinant proteins were purified using a single affinity-chromatography step in Sepharose CL-6B Ni-NTA column (Qiagen). The protein was retained within the column and it was eluted with 10 mM Tris, 200 mM imidazole, pH 8.0. The presence of FIV-rp24 was monitored by SDS-PAGE throughout the purification. The protein concentration was determined spectrophotometrically by using the extinction coefficients at 280 nm [17].

2.3. Circular dichroism measurements

Circular dichroism (CD) spectra were obtained on a Jasco J-715 spectropolarimeter using a 0.1 cm pathlength cell at 25 °C. The temperature in the cuvette was regulated with a Neslab RT-11 circulating water bath. The protein concentration was 0.1-0.15 mg/ml. The buffer used was 10 mM sodium phosphate, pH 7.0. A minimum of four spectra were accumulated for each sample and the contribution of the buffer was always subtracted. The resultant spectra were smoothed using J715 Noise Reduction software. The values of mean residue molar ellipticities [Θ] (degrees x cm^2 x $dmol^{-1}$) were calculated on the basis of 113 as the average M_r per residue.

2.4. Fluorescence measurements

Fluorescence studies were carried out on a SLM Aminco 8000C spectrofluorimeter, fit with a 450 W xenon arc. A 0.4 cm excitation pathlength and 1 cm emission pathlength quartz cell was used. In all cases, the protein concentration was 0.1-0.15 mg/ml in a 10 mM sodium phosphate, pH 7.0 buffer. The contribution of urea to the emission spectra was always subtracted. The temperature in the cuvette, 25 °C, was maintained by a circulating water bath. Excitation was performed at 275 or 295 nm, and emission spectra measured over a range of 285-450 nm.

2.5. Equilibrium unfolding

A 10 mM sodium phosphate, pH 7.0 buffer, containing 1 mM Tris(2-carboxyethil) phosphine, was used throughout the unfolding experiments. Equilibrium unfolding was performed by adding a concentrated solution of either FIV-rp24 wild-type or tryptophan mutants to a series of urea concentrations in buffer at a final concentration of 0.1-0.15 mg/ml. These solutions were incubated for 4 or16 h at 4 °C. The unfolding was monitored by circular dichroism and emission fluorescence. The denaturation curves were obtained from the changes in molar ellipticity at 220 nm ($[\Theta]_{220}$) and from the shift of the wavelength of the maximum of the fluorescence emission spectrum (λ_{max}) obtained upon excitation at 275 or 295 nm.

The CD and fluorescence equilibrium unfolding data were converted to the apparent fraction of the unfolded protein (F_{app}) and plotted versus urea concentration as defined by:

$$F_{app} = (Y_{obs} - Y_N) / (Y_U - Y_N) \quad (1)$$

where Y_{obs} is the observed value of the parameter ($[\Theta]_{220}$ or λ_{max}) at an urea concentration in the region where the protein is unfolding. Y_N and Y_U are the values of the parameter for native and unfolded forms, respectively. The effect of urea on the values of Y_N and Y_U in the transition region was taken into account and was measured by determining their values at each urea concentration by linear extrapolation of the native and unfolded baselines as previously described [19,20].

In order to obtain quantitative thermodynamic parameters for the unfolding

process, the equilibrium unfolding plots were fit to either a two- or three-state model according to the denaturing binding model [18]. For a two-state model, only unfolded (*U*) and native (*N*) proteins are considered and it is assumed that the equilibrium constant depends linearly on urea concentration [18]:

$$K_{app} = K^{H_2O} \ (1 + ka)^{\Delta n} \qquad (2)$$

where K_{app} is the apparent equilibrium constant at a urea activity, *a*, K^{H_2O} is the equilibrium constant in the absence of urea, Δn is the difference in the number of binding sites for urea between the native and the unfolded forms of the protein and *k* is the binding constant of urea to the protein and its value was taken to be 0.1 [18]. The urea activity was calculated as previously described [21].

For a three-state model besides *N* and *U* an intermediate state (*I*) was considered. The equation used to fit the data was [18]:

$$K_{app} = [\ K_1K_2 + Z\ K_1] \ / \ [\ 1 + (\ 1- Z\ )\ K_1] \qquad (3)$$

where K_{app} is the apparent equilibrium constant and the equilibrium constants K_1 and K_2 are assumed to depend on urea according to Eq. 2. The parameter *Z* is the fractional change in the ellipticity value in the transition from *N* to *I* and is defined as $Z = (Y_I - Y_N) / (Y_U - Y_N)$ where Y_I is the value of the ellipticity for the intermediate state. A nonlinear least-squares program from Sigma Plot, which uses the Marquardt-Levenberg algorithm [22], was employed to estimate the parameters of Eq. 3.

3. Results

3.1. Spectroscopic features of FIV-rp24 and mutant proteins in 9 M urea

The three-dimensional structure of FIV-rp24 provides an asymmetric environment to the aromatic residues which gives rise to a near-UV CD spectrum that is a complex combination of multiple Cotton effects [17]. Moreover, the far-UV CD spectra of FIV-rp24 and tryptophan mutants are characteristic of a protein with a high content in α-helix [17]. In the presence of 9 M urea the CD features of recombinant FIV-p24 and its Trp mutants are those of a fully unfolded protein. Thus, the near-UV CD spectra are coincident with the baseline, indicative of the absence of an asymmetric environment for the aromatic amino acids, and the far-UV CD spectra up to 210 nm are indicative of a high proportion of disordered secondary structure (data not shown).

On the other hand, the fluorescence emission spectra of native FIV-rp24 and mutant proteins indicate that the tryptophan residues occupy a highly hydrophobic environment in the three-dimensional structure, being the emission maximum for tryptophan residues of all these proteins located at around 320-322 nm [17]. However, when the proteins are dissolved in 9 M urea there was a considerable conformational change that altered the tryptophan environment. The fluorescence emission spectra obtained upon excitation at 275 and 295 nm of wild-type and mutants proteins in the presence of 9 M urea are depicted in Fig.1. Upon excitation at 275 nm FIV-rp24 wild-type and W40F and W126F mutants show two maxima at 300 and 340 nm. Since the positions of the emission

maximum for Tyr and Trp in solution are 300 and 348-350 nm respectively [23], the two maxima observed must correspond to these two amino acids although the tyrosine contribution shifts that of tryptophan to a lower wavelength. In fact, when the excitation was performed at 295 nm the maximum is observed at 346-347 nm (Fig. 1A-C). The emission spectrum of the double mutant (Fig. 1D) provides the contribution of tyrosine residues to the emission of FIV-rp24 which is virtually equal to that observed for the two single mutants (Fig. 1B and C) and not too different to that of the wild-type protein (Fig. 1A). Upon urea-induced unfolding, there is a coincidence of the emission spectra of the two single mutants, indicative that Trp40 and Trp126 are then in a similar polar environment and that the resonance energy transfer from tyrosine to tryptophan residues that takes place in the native proteins [17] is lost in the presence of urea.

3.2. Equilibrium Unfolding

From the observations mentioned above it is clear that FIV-rp24 and mutant proteins are denatured in the presence of 9 M urea. Dilution of denatured samples to a urea concentration lower than 3 M yielded proteins with both CD and fluorescence spectra indistinguishable from those of native proteins. Thus the urea-induced unfolding transition is 100% reversible. To follow unfolding CD and fluorescence spectroscopy were used after incubating FIV-rp24 and mutant proteins with different urea concentrations for 4 h at 4 °C to assure that the system had reach the equilibrium; incubation for longer time, up to 16 h, did not modify the spectral properties any further. The denaturation process was monitored by

measuring the ellipticity at 220 nm and the position of the fluorescence emission maximum upon excitation at 275 nm (Fig. 2). The high absorption of urea hindered to obtain the CD spectra at a wavelength lower than 210 nm and hence 220 nm was chosen to follow the unfolding process. On the other hand, although usually solvent exposure of Trp lowers its quantum yield [23], denaturation of FIV-rp24 and Trp mutants induced an increase in the fluorescence intensity. As stated for other proteins [24], this fact must be due to the quenching of Trp fluorescence in the native structure by side chains that are close in the folded state but widely spaced in the unfolded state. The increase in fluorescence intensity could not be used to follow unfolding because of the inconsistency and high dependence of the fluorescence intensity with urea concentration. However, the shift in the position of the emission maximum, from 320 to 340 nm, allowed to easily follow the unfolding process of native and single mutant proteins. In the case of the double mutant the shift was from 298 to 303 nm but also allowed to obtain consistent denaturation curves.

Up to 3.5 M urea there was a slight decrease in the ellipticity value that accounts for the small effect of urea on the secondary structure of the native conformation (Fig. 2A). From this concentration, a marked increase from -16000 to -2000 degrees x cm^2 x $dmol^{-1}$ in the ellipticity value was observed (Fig. 2A). The shape of the curve is indicative of both a highly cooperative loss of secondary structure and of the existence of more than one transition. Moreover, the fluorescence properties were maintained constant up to 5 M urea, and from this concentration a sharp shift in the position of the maximum was observed (Fig. 2B), but only one transition was evident. The results shown are those obtained for the

wild type protein but, as indicated below, similar results were obtained for all the mutants.

In order to compare the transitions monitored by both spectroscopic properties, the equilibrium fraction unfolded ratio at increasing urea concentrations for the wild-type protein and tryptophan mutants was determined from both CD and fluorescence spectroscopy data, as indicated in the Materials and methods section. Linear extrapolation of the ellipticity values at low and high urea concentrations allowed the determination of Y_N and Y_U in the unfolding region. This correction was not necessary when fluorescence spectroscopy was used to follow denaturation since the effect of urea in the emission maximum of native and unfolded forms is almost nil. Analysis of the urea denaturation process for both the wild-type and mutant proteins by CD techniques (measurement of $[\Theta]_{220}$) rendered highly cooperative behaviors (experimental data in Fig. 3). In spite of the difference in the urea midpoint, which is explained below, the behavior of all the proteins against urea denaturation is similar which indicates that in terms of secondary structure there is little difference in the unfolding pattern between the wild-type and mutant proteins. In all four cases a well-defined shoulder in the sigmoidal curves is observed. This discontinuity strongly suggests the presence of three species involved in the unfolding process: the native protein (*N*), the unfolded protein (*U*), and an unfolding intermediate (*I*). Table 1 shows the urea concentration values at the midpoints of the first and second transition which occur during the unfolding process. The first transition occurs at a urea concentration that is very similar for both the wild-type and mutant proteins (3.9-4.2 M). However, for the second transition this concentration is shifted from 6.2 M urea for

the wild-type protein and W40F mutant to ~5.2 M urea for W126F mutant and the double mutant. Consequently, both W126F and the double mutant seem to be less stable towards urea denaturation than FIV-rp24 and W40F. These results are in agreement with previous thermal denaturation studies [17] that showed that the mutants W126F and W40/126F were thermally less stable than the wild-type protein and the mutant W40F and which pointed towards a higher contribution of Trp126 to the stabilization of the three-dimensional structure. In any case, the stability against urea denaturation of these four proteins is higher than that of HIV-1 p24 that has been shown to have a single transition with a midpoint at 3.4-3.9 M urea [16].

Analysis of the unfolding curves followed by fluorescence spectroscopy (shift in the emission maximum) (Fig. 4) indicates that there is only one highly cooperative transition for both wild-type and mutant proteins. Moreover, the urea concentration at the midpoint of this transition was coincident with the urea concentration corresponding to the second transition observed by CD (Table 1). Additionally, identical results were obtained upon excitation at 295 nm (data not shown). The absence of the discontinuity indicates that when the unfolding is monitored by fluorescence only two species are detectable. The most likely explanation to these data relies in the assumption that in the intermediate folding state (*I*) the environment of both Trp40 and Trp126 is still unaffected. A further increase in the urea concentration from this intermediate folding state leads to a second structural transition, with similar midpoints when monitored by fluorescence and CD, indicative of a structural change in which now both Trp40 and Trp126 are involved.

3.3. Analysis of the denaturation curves

Mathematical analysis of the urea-induced unfolding curves was performed in terms of the denaturing binding model [18], by fitting the CD denaturation curves to a three-state model (Fig. 3, solid lines) and the fluorescence denaturation curves to a two-state model (Fig. 4, solid lines). As it can be seen there is good agreement between the theoretical and the experimental data. The thermodynamic parameters calculated from these fits are shown in Tables 2 and 3. The fitting routine used may not adequately consider correlation between the fitting parameters, so the reported standard deviations for the fits may be underestimates. The free energy change in the absence of urea for the first transition is similar for all the proteins and only slightly higher than the value corresponding to the second transition (Table 2). The difference in the number of binding sites for urea is also similar for all the proteins but it is higher between the native form and the intermediate state than between the intermediate state and the unfolded form. The *Z* parameter, defined as the fractional change in the CD signal in the transition from *N* to *I*, changed from 0.27 for the wild-type protein to 0.19 for the double mutant, indicating that, approximately, 19-27% of the total change in $[\Theta]_{220}$ observed in the complete unfolding occurs in the transition from *N* to *I*.

When the denaturing binding model was applied to the denaturation curves obtained with the maximum of the emission fluorescence spectra upon excitation at 275 nm, the thermodynamic parameters shown in Table 3 were obtained. Similar results were obtained for the denaturation followed by measuring emission

fluorescence upon excitation at 295 nm (data not shown). The quantitative analysis was performed because, except for the double mutant, the emission maxima of the native and denatured forms are well separated. Although the thermodynamic data can be affected of a big error, the results show that both the free energy change and the difference in the number of binding sites for urea are totally comparable to those of the second transition calculated from CD data, being the differences of the same order than those obtained for a protein when different spectroscopic parameters are employed [19,25]. This result was not unexpected since, as indicated above, the changes in the Trp fluorescence take place during the transition from the intermediate state to the unfolded form.

Using the thermodynamic parameters reported in Table 2, the fractions of the native (f_N), intermediate (f_I) and unfolded (f_U) forms at various urea concentrations were calculated (Fig. 5). According to this model, in the case of FIV-rp24 (Fig. 5A) the unfolding intermediate appears at 3.5 M urea, being almost the only species at 4.2 M urea. Comparison of this theoretical denaturation plot with the experimental unfolding curve obtained by CD (Fig. 3A) allows the conclusion that this is the urea concentration at which the first transition takes place (Fig. 5A). Appearance of the unfolded species (*U*) does not occur until 4 M urea, becoming the predominant form above 5.5 M urea and mostly the only remaining form at 6.5 M urea. Inspection of the theoretical denaturation plots in the case of the tryptophan mutants (Fig 5, panels B, C and D) indicates that *I* is the predominant species at 4.4 M (W40F), 4.0 M (W126F) and 3.9 M urea (W40/126), also coincident with the experimental midpoint for the first transition of the urea unfolding curves obtained by CD (Fig 3). The unfolded form appeared at 4-4.5 M

urea and at 6-6.5 M urea it was the only species observed.

4. Discussion

The mechanism by which polypeptides fold into their native conformation from an initially disorganized form is still one of the fundamental problems in structural biology. In the case of the lentiviral core proteins family few details are known about the folding mechanism [16]. To further study how these proteins fold, we have performed site directed mutagenesis in Trp residues of FIV-rp24 and urea denaturation have been carried out. Aromatic amino acids in proteins have been extensively used as sensitive intrinsic probes to monitor the unfolding, refolding and the stability of polypeptide chains [see 25-28 for a few examples].

FIV-rp24 has two Trp residues at positions 40 and 126, of which Trp40 is not conserved in the rest of lentiviral core proteins [1-4]. This suggests that at least this Trp residue does not play a critical role in the maintenance of the three-dimensional structure and hence can be changed without altering significantly the overall structure. CD and emission fluorescence data indicate that replacement of one or two tryptophan residues by phenylalanine affects neither the protein secondary structure nor the three-dimensional structure [17], being the small changes induced by the substitutions restricted to the locations of the mutations. Urea was chosen to unfold the wild-type and mutant proteins. In the presence of 9 M urea their CD and fluorescence spectra are coincident with those of a fully unfolded protein. The two spectroscopic parameters employed to follow unfolding were the ellipticity at 220 nm and the shift in the fluorescence emission maximum. Since the aromatic side chains do not contribute to FIV-rp24 far-UV spectrum [17], the variations in $[\Theta]_{220}$ must reflect changes in secondary structure.

On the other hand, the changes in fluorescence should reflect changes in the local Trp environment since the maximum at 320 nm is due to Trp residues and similar results were obtained upon excitation at 295 nm, wavelength that enables to isolate the Trp fluorescence [23]. Inspection of the urea-induced denaturation curves shows that there is a first transition for all the proteins that is registered by CD measurements but is not observed by fluorescence, and a second transition that is observed by both CD and fluorescence. Therefore, in the first transition part of the secondary structure is modified without being altered the Trp environment. Since both tryptophan residues are in the amino-terminal domain of the core protein, the first unfolding transition most likely reflects the denaturation of the carboxy-terminal region of FIV-rp24. Consequently, the second transition should reflect the denaturation of the amino-terminal domain.

The existence of two transitions would be indicative of the presence of at least one stable intermediate state that accumulates under unfolding equilibrium conditions. According to CD data [17], the predominant element of secondary structure of FIV-rp24 is α-helix, representing about 53% of the secondary structure elements. This percentage is the same as that of EIAV-p26 [8] and HIV-p24 [9] deduced from their crystal structure. Most of the helix (70%) is located in the amino-terminal domain and the remainder (30%) in the carboxy-terminal domain. Since the parameter Z, the fractional change in the ellipticity value in the transition from *N* to *I*, has a value of 0.27-0.19 depending on the protein, the intermediate state observed in the denaturation process would have a 73-81% of the ellipticity at 220 nm. If we consider that the ellipticity at 220 nm is a measure of the α-helical content of the protein, the intermediate state, with the N-terminal domain folded,

would have a 73-81% of α-helix structure, a value similar to the calculated contribution of the amino-terminal domain to FIV-rp24 secondary structure. On the other hand, since the two mutated tryptophan residues are far in the three-dimensional structure and both W40F and W126F mutants seem to unfold through a similar intermediate, the existence of further unfolding intermediates within the amino-terminal domain can be ruled out. The denaturation data of these two single mutants, obtained by different spectroscopical techniques, are coincident indicating that the unfolding of this domain follows an all-nothing mechanism, without intermediate states.

The free energy change in the absence of denaturant can be considered as a measure of a protein conformational stability, being the mean value, as determined by equilibrium unfolding, 10.8 ± 3.6 kcal/mol [29]. Although there is considerable error in the estimations of the free energy changes for *U* to *I* and *I* to *N*, some conclusions may be drawn from these values. The ΔG^{H_2O} values for both N- and C-terminal domains are on the upper limit of the conformational stability of globular proteins. Moreover, it is of the same order than the value described for small proteins like barnase (110 residues, 8.7 kcal/mol) [30] or ribonuclease A (124 residues, 9.3 kcal/mol) [31] or for isolated domains like the C-terminal domain of γB-crystallin (8.6 kcal/mol) [15] or the 111-residue domain of the murine cellular prion protein (7.0 kcal/mol) [32]. Additionally, both values are considerably higher than that derived for the only transition observed for HIV-1 rp24 which is in the range 4.3-5.8 kcal/mol [16].

For a number of proteins it has been shown that the properties of the intermediates observed by equilibrium unfolding-refolding studies are similar to

those of the transient intermediates detected during unfolding kinetic studies [33-36]. If this is the case for FIV-rp24, and the intermediate is a productive intermediate on the unfolding pathway, the denaturation data described herein can reflect the loss of structure of the two domains in a sequential and independent way. These unfolding data could somehow explain the appearance of a molten globule in the case of HIV-1 rp24 [16] since the molten globule state may be analogous to a partly folded state of a protein composed of several domains in which some are folded and other unfolded [37]. Finally, since the unfolding process is reversible, it could be hypothesized that the two domains behave as independent folding units and that the mechanism of folding of FIV-rp24 would consist of two steps. Starting with an unfolded polypeptide, in a first step the amino-terminal region would adopt its native structure, and in a second step the carboxy-terminal domain would eventually fold.

Acknowledgements

This work was supported by Grants from the DGES (Spain) (PB96-0602) and from the NIH (USA) (AI15955).

References

[1] R.M. Stephens, J.W. Casey, N.R. Rice, Equine infectious anemia virus *gag* and *pol* genes: relatedness to visna and AIDS virus, Science 231 (1986) 589-594.

[2] R.A. Olmsted, V.M. Hisch,, R.H. Purcell, P.R. Johnson, Nucleotide sequence analysis of feline immunodeficiency virus: genome organization and relationship to other lentiviruses, Proc. Natl. Acad. Sci. USA 86 (1989) 8088-8092.

[3] R.L. Talbott, E.E. Sparger, K.M. Lovelace, W.M. Fitch, N.C. Pedersen, P.A. Luciw, J.H. Elder, Nucleotide sequence and genomic organization of feline immunodeficiency virus, Proc. Natl. Acad. Sci. USA 86 (1989) 5743-5747.

[4] J.W. Wills, R.C. Craven, Form, function, and use of retroviral gag proteins. AIDS 5 (1991) 639-654.

[5] C. Momany, L.C. Kovari, A.J. Prongay, W. Keller, R.K. Gitti, B.M. Lee, A.E. Gorbalenya, L. Tong, J. McClure, L.S. Ehrlich, M.F. Summers, C. Carter, M.G. Rossmann, Crystal structure of dimeric HIV-1 capsid protein, Nat. Struct. Biol. 3 (1996) 763-770.

[6] R.K. Gitti, B.M. Lee, J. Walker, M.F. Summers, S. Yoo, W.I. Sundquist, Structure of the amino-terminal core domain of the HIV-1 capsid protein, Science 273 (1996) 231-235.

[7] T.R. Gamble, S. Yoo, F.F. Vadjos, U.K. von Schwedler, D.K. Worthylake, H. Wang, J.P. McCutcheon, W.I. Sundquist, C.P. Hill, Structure of the carboxyl-terminal dimerization domain of the HIV-1 capsid protein, Science

278 (1997) 849-852.

[8] Z. Jin, L. Jin, D.L. Peterson, C.L. Lawson, Model for lentivirus capsid core assembly based on crystal dimers of EIAV p26, J. Mol. Biol. 286 (1999) 83-93.

[9] C. Berthet-Colominas, S. Monaco, A. Novelli, G. Sibaï, F. Mallet, S. Cusack, Head-to-tail dimers and interdomain flexibility revealed by the crystal structure of HIV-1 capsid protein (p24) complexed with a monoclonal antibody Fab, EMBO J. 18 (1999) 1124-1136.

[10] S.D. Fuller, T. Wilk, B.E. Gowen, H.-G. Kräusslich, V.M. Vogt, Cryo-electron microscopy reveals ordered domains in the immature HIV-1 particle, Curr. Biol. 7 (1997) 729-738.

[11] E.K. Franke, H.E.H. Yuan, K.L. Bossolt, S.P. Goff, J. Luban, Specificity and sequence requirements for interactions between various retroviral gag proteins. J. Virol. 68 (1994) 5300-5305.

[12] A.S. Reicin, S. Paik, R.D. Berkowitz, J. Luban, I. Lowy, S.P. Goff, Linker insertion mutations in the human immunodeficiency virus type 1 gag gene: effects on virion particle assembly, release, and infectivity. J. Virol. 69 (1995) 642-650.

[13] C.T. Wang, E. Barklis, Assembly, processing, and infectivity of human immunodeficiency virus type 1 gag mutants. J. Virol. 67 (1993) 4264-4273.

[14] U.K. von Schwedler, T.L. Stemmler, V.Y. Klishko, S. Li, K.H. Albertine, D.R. Davis, W.I. Sundquist, Proteolytic refolding of the HIV-1 capsid protein amino-terminus facilitates viral core assembly, EMBO J. 17 (1998) 1555-1568.

[15] E.-M. Mayr, R. Jaenicke, R. Glockshuber, The domains in γB.crystallin: identical fold-different stabilities, J. Mol. Biol. 269 (1997) 260-269.

[16] R. Misselwitz,, G. Hausdorf, K. Welfle, W.E. Höhne, H. Welfle, Conformation and stability of recombinant HIV-1 capsid protein p24 (rp24), Biochim. Biphys. Acta 1250 (1995) 9-18.

[17] B. Yélamos, E. Núñez, J. Gómez-Gutiérrez, M. Datta, B. Pacheco, D.L. Peterson, F. Gavilanes, Circular dichroism and fluorescence spectroscopic properties of the major core protein of feline immunodeficiency virus and its tryptophan mutants. Assignment of the individual contribution of the aromatic side chains, Eur. J. Biochem. 266 (1999) 1081-1089.

[18] C. Tanford, Protein denaturation, Adv. Protein Chem. 24 (1970) 1-95.

[19] C.R. Matthews, M.M. Crisanti, Urea-induced unfolding of the α subunit of tryptophan synthase: evidence for a multistate process, Biochemistry 20 (1981) 784-792.

[20] J.F. Cupo, C.N. Pace, Conformational stability of mixed disulfide derivatives of β-lactoglobulin B, Biochemistry 22 (1983) 2654-2658.

[21] C.N. Pace, Determination and analysis of urea and guanidine hydrochloride denaturation curves, Methods Enzymol. 131 (1986) 266-280.

[22] W.H. Press, B.P. Flannery, S.A. Teukolsky, W.T. Vetterling, in: Numerical Recipes, Cambridge University Press, Cambridge, (1986).

[23] J.R. Lakowicz, in: Principles of fluorescence spectroscopy, 2nd edition, Kluwer Academic/Plenum Publishers, New York, (1999), pp.445-486.

[24] B.K. Szpikowska, J.M. Beechem, M.A. Sherman, M.T. Mas, Equilibrium unfolding of yeast phosphoglycerate kinase and its mutants lacking one or

both native tryptophans: a circular dichroism and steady-state and time-resolved fluorescence study, Biochemistry 33 (1994) 2217-2225.

[25] M.A. Sherman, J.M. Beechem, M.T. Mas, Probing intradomain and interdomain changes during equilibrium unfolding of phosphoglycerate kinase: fluorescence and circular dichroism study of tryptophan mutants, Biochemistry 34 (1995) 13934-13942.

[26] K. Cai, V. Schirch, Structural studies on folding intermediates of serine hydroxymethyltransferase using single tryptophan mutants, J. Biol. Chem. 271 (1996) 2987-2994.

[27] X. Shao, C.R. Matthews, Single-tryptophan mutants of monomeric tryptophan repressor: optical spectroscopy reveals nonnative structure in a model for an early folding intermediate, Biochemistry 37 (1998) 7850-7858.

[28] F.W. West, H.-S. Seo, T.D. Bradrick, E.E. Howell, Effects of single-tryptophan mutations on R67 dihydrofolate reductase, Biochemistry 39 (2000) 3678-3689.

[29] R. Jaenicke, Stability and folding of domain proteins, Prog. Biophys. Mol. Bio. 71 (1999) 155-241.

[30] C.N. Pace, D.V. Laurents, R.E. Erickson, Urea denaturation of barnase: pH dependence and characterization of the unfolded state, Biochemistry 31 (1992) 2728-2734.

[31] C.N. Pace, Measuring and increasing protein stability, Trends Biotechnol. 8 (1990) 93-98.

[32] G. Wildegger, S. Liemann, R. Glockshuber, Extremely rapid folding of the C-terminal domain of the prion protein without kinetic intermediates, Nat.

Struct. Biol. 6 (1999) 550-553.

[33] D. Hamada, Y. Goto, The equilibrium intermediate of β-lactoglobulin with non-native α-helical structure, J. Mol. Biol. 269 (1997) 479-487.

[34] K. Fujiwara, M. Arai, A. Shimizu, M. Ikeguchi, K. Kuwajima, S. Sugai, Folding-unfolding equilibrium and kinetics of equine β-lactoglobulin: equivalence between the equilibrium molten globule state and a burst-phase folding intermediate, Biochemistry 38 (1999) 4455-4463.

[35] M. Mizuguchi, M. Arai, Y. Ke, K. Nitta, K. Kuwajima, Equilibrium and kinetics of the folding of equine lysozyme studied by circular dichroism spectroscopy, J. Mol. Biol. 283 (1998) 265-277.

[36] J.M. Beechem, M.A. Sherman, M.T. Mas, Sequential domain unfolding in phosphoglycerate kinase: fluorescence intensity and anisotropy stopped-flow kinetics of several tryptophan mutants, Biochemistry 34 (1995) 13943-13948.

[37] E. Freire, Thermodynamics of partly folded intermediates in proteins, Annu. Rev. Biophys. Biomol. Struc. 24 (1995) 141-165.

Figure Legends

Fig. 1. Fluorescence emission spectra of FIV-rp24 and its Trp mutants in the presence of 9 M urea. The emission spectra were recorded between 285 and 450 nm for an excitation wavelength of 275 nm (continuous line) and between 305 and 450 nm for an excitation wavelength of 295 nm (dashed line) nm. In all cases, the protein concentration was 0.15 mg/ml. The buffer used was 10 mM sodium phosphate buffer, pH 7.0, 9 M urea. The wild-type protein is shown in panel A, mutant W40F in panel B, mutant W126F in panel C and the double mutant W40/126F in panel D.

Fig. 2. Equilibrium unfolding curve for wild-type FIV-rp24 as monitored by circular dichroism (A) and fluorescence spectroscopy (B). A, variation of the molar ellipticity value at 220 nm ($[\Theta]_{220}$) with increasing urea concentrations. The dashed lines show the assumed solvent perturbation effect on the ellipticity values of the native and unfolded forms at varying urea concentrations. B, wavelength (nm) of the fluorescence emission maximum (λ_{max}) upon excitation at 275 nm as a function of urea concentration.

Fig. 3. Equilibrium unfolding curves for FIV-rp24 and its single and double Trp mutants as monitored by CD. A, FIV-rp24, B, W40F, C, W126F, D, W40/126F. The CD spectra of a 0.15 mg/ml solution of the different proteins were monitored at increasing urea concentrations. The ellipticity at 220 nm was used to calculate the unfolded fraction (F_{app}) as described in the Materials and methods section. The

continuous lines are the fit of the experimental data to a three-state model [18].

Fig. 4. Equilibrium unfolding curves for FIV-rp24 and its single and double Trp mutants as monitored by fluorescence spectroscopy. A, FIV-rp24; B, W40F; C, W126F; D, W40/126F. The position of the fluorescence emission maximum upon excitation at 275 nm was measured as a function of the urea concentration. The protein concentration employed was 0.15 mg/ml. The data were plotted as the fraction unfolded (F_{app}) as determined in the Materials and methods section. The continuous lines are the fit of the experimental data to a two-state model [18].

Fig. 5. Calculated fraction (*f*) of the native, intermediate and unfolded forms of the wild-type protein and Trp mutants. A, FIV-rp24; B, W40F; C, W126F; D, W40/126F. Symbols for different proteins are: *filled circles,* native form; *filled squares*, intermediate state; *filled triangles*, unfolded form. The data employed to calculate the fraction of the different forms were obtained from the fit of the denaturation curves monitored by CD.

Table 1

Molar urea concentrations at midpoints observed in the denaturation curves of FIV-rp24, W40F, W126F and W40/126F.

	CD[a]		F_{275}[b]
	1st transition	2nd transition	
FIV-rp24	4.2 ± 0.1	6.2 ± 0.3	6.4 ± 0.1
W40F	4.3 ± 0.1	6.2 ± 0.1	6.5 ± 0.4
W126F	4.0 ± 0.1	5.3 ± 0.2	5.3 ± 0.3
W40/126F	3.9 ± 0.1	5.2 ± 0.3	4.6 ± 0.4

[a] Denaturation curves followed by measuring the molar ellipticity at 220 nm.

[b] Denaturation curves followed by measuring the shift in the emission maximum upon excitation at 275 nm.

Table 2

Thermodynamic parameters for the unfolding equilibrium of FIV-rp24 and its Trp mutants calculated from the denaturation curves monitored by CD. These values were obtained by fitting the denaturation curves to a three-state model [18].

	$\Delta G_1^{H_2O}$ (kcal mol^{-1}) [a]	$\Delta G_2^{H_2O}$ (kcal mol^{-1}) [b]	Δn_1 [c]	Δn_2 [d]	Z [e]
FIV-rp24	12.04 ± 0.33	8.47 ± 1.30	63.73 ± 2.70	34.85 ± 2.30	0.27 ± 0.05
W40F	12.14 ± 0.15	10.50 ± 0.50	65.00 ± 0.50	40.05 ± 2.40	0.25 ± 0.04
W126F	12.01 ± 0.13	10.42 ± 0.76	68.88 ± 0.40	45.12 ± 2.20	0.21 ± 0.06
W40/126F	11.79 ± 0.11	10.09 ± 0.34	69.91 ± 3.41	45.35 ± 0.98	0.19 ± 0.04

[a] $\Delta G_1^{H_2O}$, free energy change corresponding to the transition from the native protein to the intermediate state.

[b] $\Delta G_2^{H_2O}$, free energy change corresponding to the transition from the intermediate state to the unfolded protein.

[c] Δn_1, difference in the number of binding sites for urea between the native and the intermediate state.

[d] Δn_2, difference in the number of binding sites for urea between the intermediate state and the unfolded protein.

[e] *Z*, fractional change in the ellipticity value in the transition from the native protein to the intermediate state.

Table 3

Thermodynamic parameters for the unfolding equilibrium of FIV-rp24 and its Trp mutants calculated from the denaturation curves monitored by fluorescence spectroscopy. These values were obtained by fitting the denaturation curves to a two-state model [18].

	ΔG^{H_2O}(kcal mol^{-1}) [a]	Δn [b]
FIV-rp24	11.95 ± 0.19	43.43 ± 0.85
W40F	12.01 ± 1.22	42.53 ± 2.04
W126F	12.90 ± 0.82	51.94 ± 0.96
W40F/W126F	8.14 ± 0.30	39.97 ± 1.50

[a] ΔG^{H_2O}, free energy change corresponding to the transition from the native protein to the unfolded protein.

[b] Δn, difference in the number of binding sites for urea between the native and the unfolded protein.

Figure 1

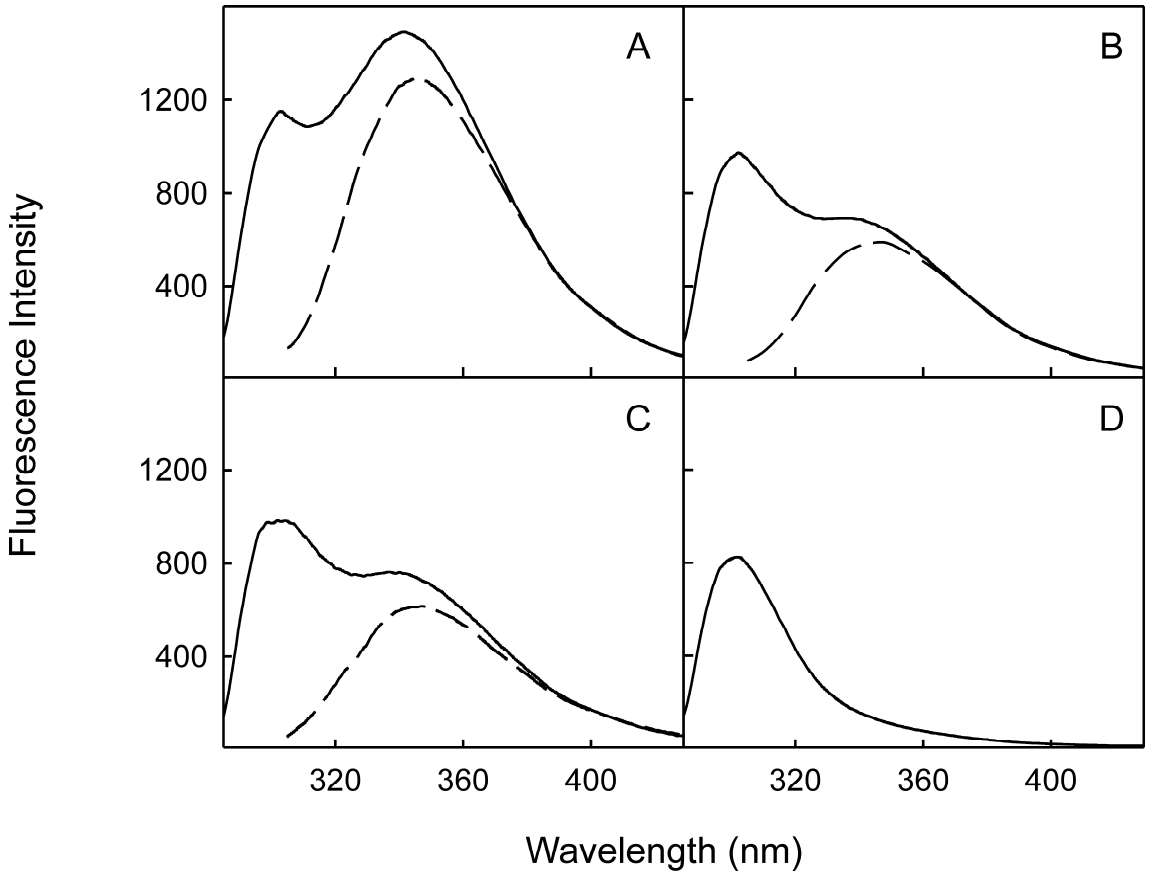
A
B
C
D
1200
800
400
1200
800
400
320
360
400
320
360
400
Fluorescence Intensity
Wavelength (nm)

Figure 2

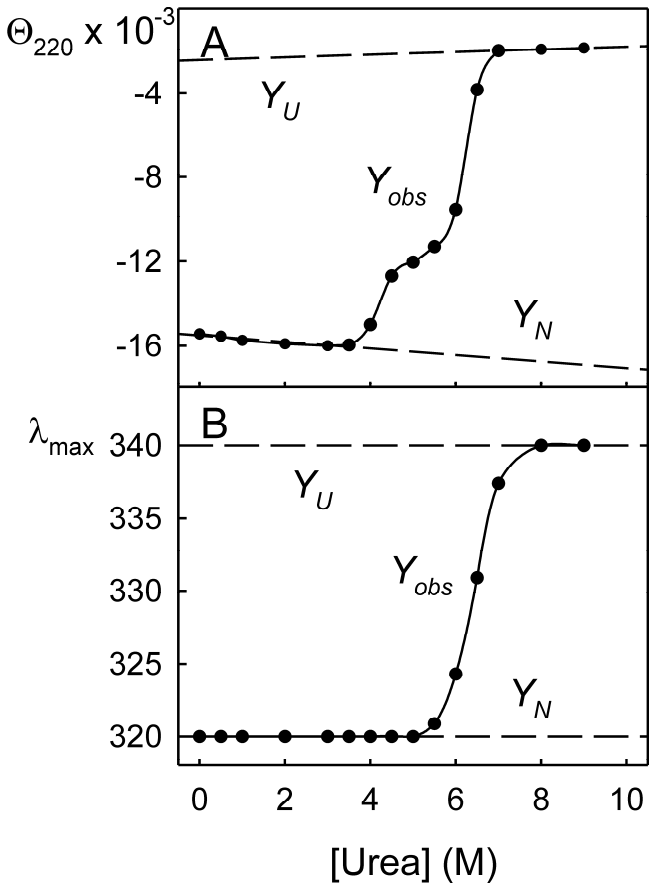
Θ220 x 10-3
A
YU
Yobs
YN
-4
-8
-12
-16
λmax
B
340
335
330
325
320
0
2
4
6
8
10
[Urea] (M)

Figure 3

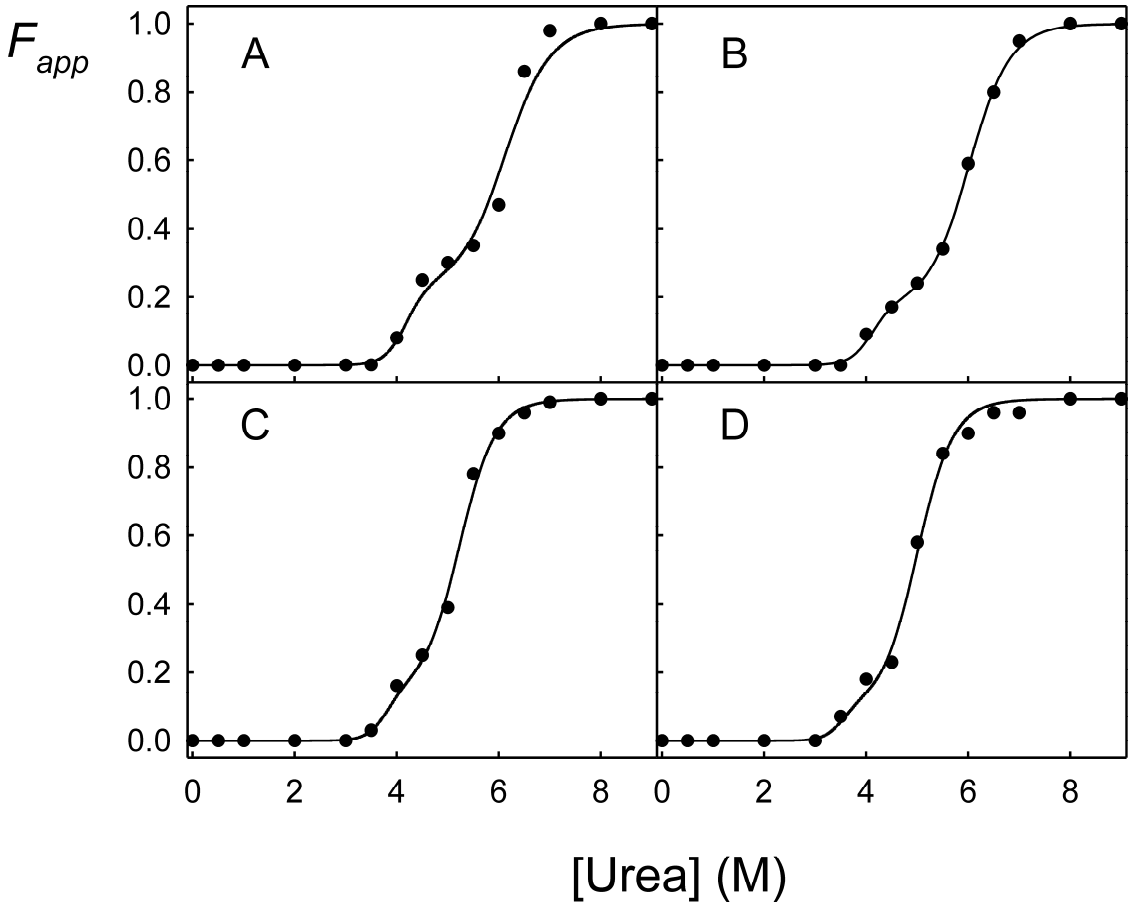

Figure 4

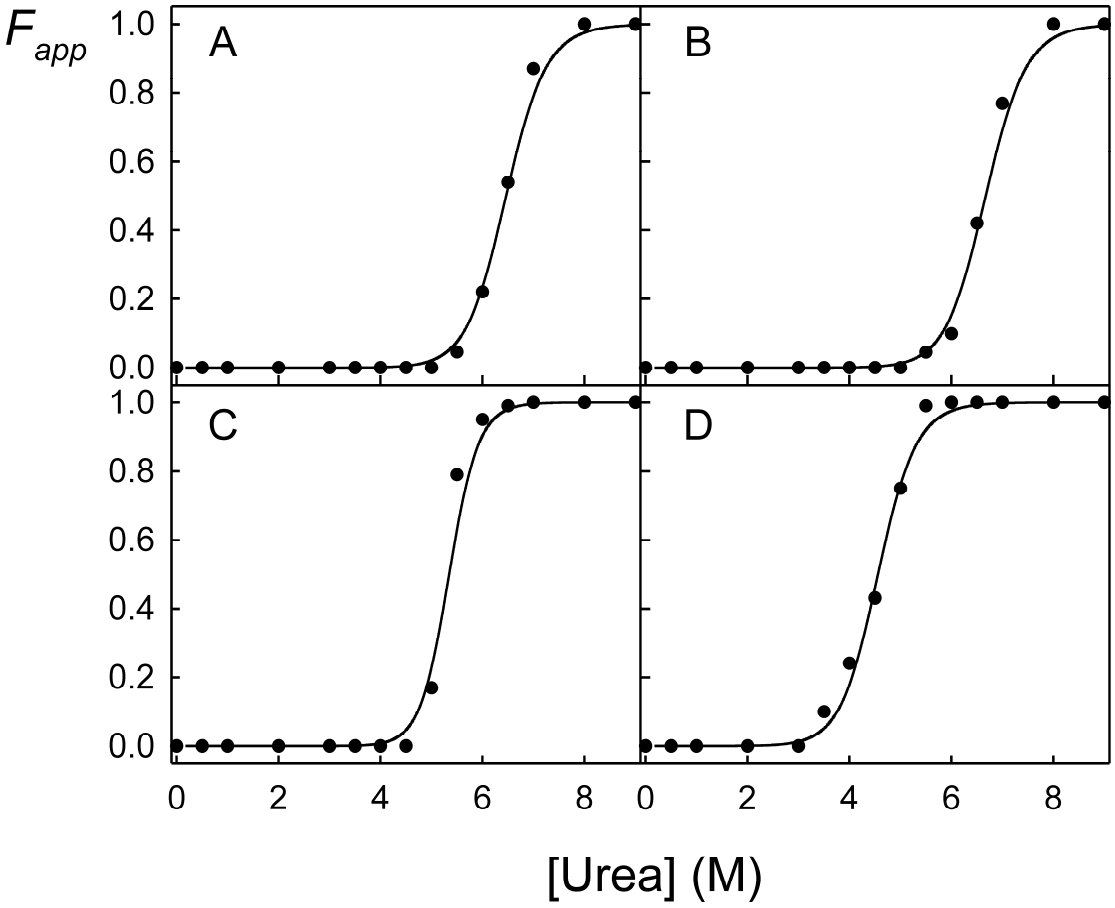

Figure 5